Supporting Information for

"Diluting branches" put to work: from synthesis to properties control of multifunctional polymers derived from triphenylamine, fluorene and thiophene

Ioana-Alexandra Trofin, Catalin-Paul Constantin, Mariana-Dana Damaceanu, Radu-Dan Rusu*

Petru Poni Institute of Macromolecular Chemistry, Romanian Academy, Electroactive Polymers and Plasmochemistry Department, Grigore Ghica Voda Alley, 41A, Iasi, 700487, Romania

Experimental section

Starting materials. All starting compounds, catalysts, and salts used during synthesis, and all chemicals and indium tin oxide-coated glass (ITO, surface resistivity 30–60 $\Omega \cdot sq^{-1}$) substrates involved in electrochemical experiments are commercially available reagents. Except for 2,5-dibromo-3-octylthiophene (synthesis presented below), they were purchased from Sigma Aldrich or TCI and used without further purification. All solvents were acquired from Roth or TCI as of UV or IR grade and were used as received.

Synthesis of 2,5-dibromo-3-octylthiophene.2,5-Dibromo-3-octylthiophene was synthesized based on a protocol reported by the literature:[1] a solution of 3-octylthiophene (0.67 g, 34 mmol) in DMF (10 mL) was charged in a 500 mL, three-necked, round-bottomed flask (equipped with a magnetic stirring bar, nitrogen inlet and outlet, and condenser). A solution of *N*-bromosuccinimide (1.33 g, 74 mmol) in DMF (25 mL) was slowly added with a dropping funnel at 0°C. The mixture was stirred for 22 h under nitrogen in the absence of light. The reaction was quenched with water and extracted with diethyl ether (3 × 20 mL), and the resulting organic layers were washed with water and brine and dried over Na_2SO_4. The solvent was evaporated under reduced pressure, and the final product was obtained as a yellow oil (85%, 1.24 g). ^{1}H NMR ($CDCl_3$, 400.1 MHz, 25 °C, δ (ppm): 6.77 (1H, s, H9), 2.54–2.48 (2H, t, J=7.51 Hz, H8), 1.57–1.50 (2H, m, H7), 1.35–1.27 (10H, m, H2–H6), 0.90–0.87 (3H, t, J=6.71 Hz, H1).

The **NMR spectra** were recorded on a Bruker Avance III 400 instrument equipped with a 5 mm multinuclear inverse detection probe, operating at 400.1 MHz for ^{1}H nuclei. The chemical shifts are

reported in δ units (ppm) relative to the solvent's residual peak ($CDCl_3$, δ: 7.26 ppm). The results were analyzed with Bruker with TopSpin 4.0 operating software.

The infrared (**FT-IR**) **spectra** were obtained with an FT-IR Bruker Vertex 70 Spectrophotometer in ATR mode using powder samples. The FT-IR spectra were normalized using the specific aromatic C=C absorption peak at 1595 cm^{-1} as an internal standard.

The **average molar mass** values were assessed by gel permeation chromatography (GPC) using a ParSEC Chromatography Ver. 5.67 instrument from Brookhaven Instruments, employing refraction and UV detectors, PL Mixed C Column, and polystyrene standards of known molar mass. Measurements were performed on the soluble fraction of each polymer using 0.5% solutions in $CHCl_3$.

The **solubility** of the synthesized hyperbranched polymers was qualitatively measured by dissolution tests using 5 mg from the soluble fraction of each polymer in 0.5 mL of solvent (0.1% concentration).

Very **thin polymer films** were obtained from diluted polymer solutions (0.5% concentration) in various solvents, which were filtered through a syringe having a 0.45 µm pore-size PTFE membrane filter. The solutions were afterward drop-cast onto quartz or ITO plates, gradually heated from room temperature to the solvent's boiling point, and kept at this temperature for 2 h to remove the residual solvent. The obtained thin coatings were used for further measurements.

The **morphology** of the polymer coatings was investigated by using both scanning electron microscopy (SEM) and atomic force microscopy (AFM).

SEM micrographs were recorded with a Verios G4 UC Scanning Electron Microscope from Thermo Fisher Scientific operating at 5 kV on film samples fixed on Al stubs. All samples (coatings obtained by drop-casting) were coated with a 6 nm Pt layer using a Leica EM ACE200 Sputter Coater to ensure electrical conductivity and impede charge buildup during exposure to the electron beam.

AFM images were acquired with an Ntegra multifunctional Scanning Probe Microscope from NT-MDT Spectrum Instruments, employing an NSG10 rectangular silicon cantilever operating at 2.375 $N \cdot m^{-1}$ force constant and 169 kHz resonance frequency. The scanning was carried out on 20x20 μm^2 sizes of drop-cast coatings (the same as in SEM). AFM images were obtained with the Nova 1.1.1.19891 software and surface texture parameters were processed with the Image Analysis 3.5.0.20102 software.

The **thermal behavior** of the polymers was studied by thermogravimetric analysis performed on an STA 449 F1 Jupiter instrument from Netzsch, which allows simultaneous TG/DSC and TGA/DTA investigations. The experiments were performed under nitrogen flow, from 30 to 700 °C, at a heating speed of 10 $°C \cdot min^{-1}$, for samples with a weight between 3 and 5 mg. Differential scanning calorimetry

(DSC) experiments were carried out on the same instrument by recording a heating-cooling-heating cycle up to 300 °C in an inert atmosphere.

Computational studies were employed to evaluate the electron density distribution along the polymeric chains. The ground-state geometries of a simplified macromolecular segment (a single, theoretical, repetitive polymeric unit comprising all three building blocks) were fully optimized in vacuum, without any symmetry constraints by applying the density functional theory (DFT) with the B3LYP exchange-correlation functional and 6–31++G(d,p) basis set. The optimized geometry of the simplified structure was first used to evaluate the **molecular orbitals** (MO). Time-dependent DFT (TD-DFT) with the B3LYP/6–31++G(d,p) basis set of the optimized geometry in the ground state was used to compute the excited states and oscillator strengths for the lowest 30 singlet transitions and to generate **simulated UV–vis absorption spectra** in vacuum. The DFT and TD–DFT computations were performed using the Gaussian 16 software, while the molecular structures, HOMO and LUMO images, and simulated UV–vis spectra were rendered using the GaussView, version 6.1 software.

The electronic (**UV–vis**) **absorption** spectra were obtained at room temperature on a Shimadzu UV-1280 UV–vis spectrophotometer using freshly prepared, diluted (approx. 10^{-5} M) polymer solutions in various solvents (toluene, THF, DCM, DMF, NMP), or thin polymer films coated on quartz plates.

The **photoluminescence** (PL) spectra were registered at room temperature on a Shimadzu RF-6000 spectrofluorophotometer using freshly prepared, diluted (approx. 10^{-5} M) polymer solutions in various solvents (toluene, THF, DCM, DMF, NMP), or thin polymer films coated on quartz plates. In all cases, proper control was taken to maintain the film thickness in the same range. Based on AFM measurements, the film thickness is in the range of 1200–1300 nm for **P1** and **P2** and in the range of 1000–1100 nm for **P2** and **P3**, respectively. The **fluorescence quantum yields** (Φ_{fl}) were assessed in NMP solutions and thin films (drop-cast from toluene solutions) using an integrating sphere to ensure **absolute values** which are unaffected by any reference.[2,3]

Cyclic voltammetry (CV) measurements were performed on an Autolab PGSTAT204 Potentiostat-Galvanostat, in a conventional three-electrode electrochemical cell composed of an auxiliary electrode (Pt wire), a reference electrode ($Ag/AgClO_4$), and a working electrode (sample-covered ITO substrate or blank ITO substrate). The supporting electrolyte consisted of 10^{-1} M $LiClO_4$/acetonitrile (MeCN) or tetrabutylammonium perchlorate (TBAP)/DCM systems. Ferrocene was used as an external reference for calibration: E_{onset} = 0.31 V (MeCN) *vs.* $Ag/AgClO_4$. All experiments were carried out at a 100 $mV \cdot s^{-1}$ sweep rate in air at room temperature after purging the electrolyte solution with nitrogen. Two types of samples were used in the measurements: (i) thin polymer coatings obtained from 0.5% DCM solutions

(working electrode: sample-covered ITO substrate); (ii) model compounds' solutions (10^{-3} M) in the DCM–TBAP system (10^{-1} M) (working electrode: blank ITO substrate).

The **differential pulse voltammetry** (DPV) curves were recorded using the following parameters: 1.3 mV·s^{-1} scan rate; 50 mV modulation amplitude; 1.5 s interval; 0.2 s modulation time.

The **experimental HOMO and LUMO energy** values and the **bandgap energy** (E_g) values were estimated based on the following equations, using the oxidation (E_{onset}^{ox}) onset potential values *vs.* Ag/Ag$^+$, and the λ_{onset} values determined from the intersection of the polymer films' (obtained from DCM) UV–vis and PL spectra;[4-6] the HOMO energy for the ferrocene standard used for calibration was considered to be –4.8 eV at zero-vacuum level:

$$E_{HOMO} = E_{HOMO(Fc)} + (E_{onset(Fc)}^{Ox} - E_{onset}^{Ox}) \quad (1)$$

$$E_g = 1240/\lambda_{onset} \quad (2)$$

$$E_{LUMO} = E_g + E_{HOMO} \quad (3)$$

Results and discussions

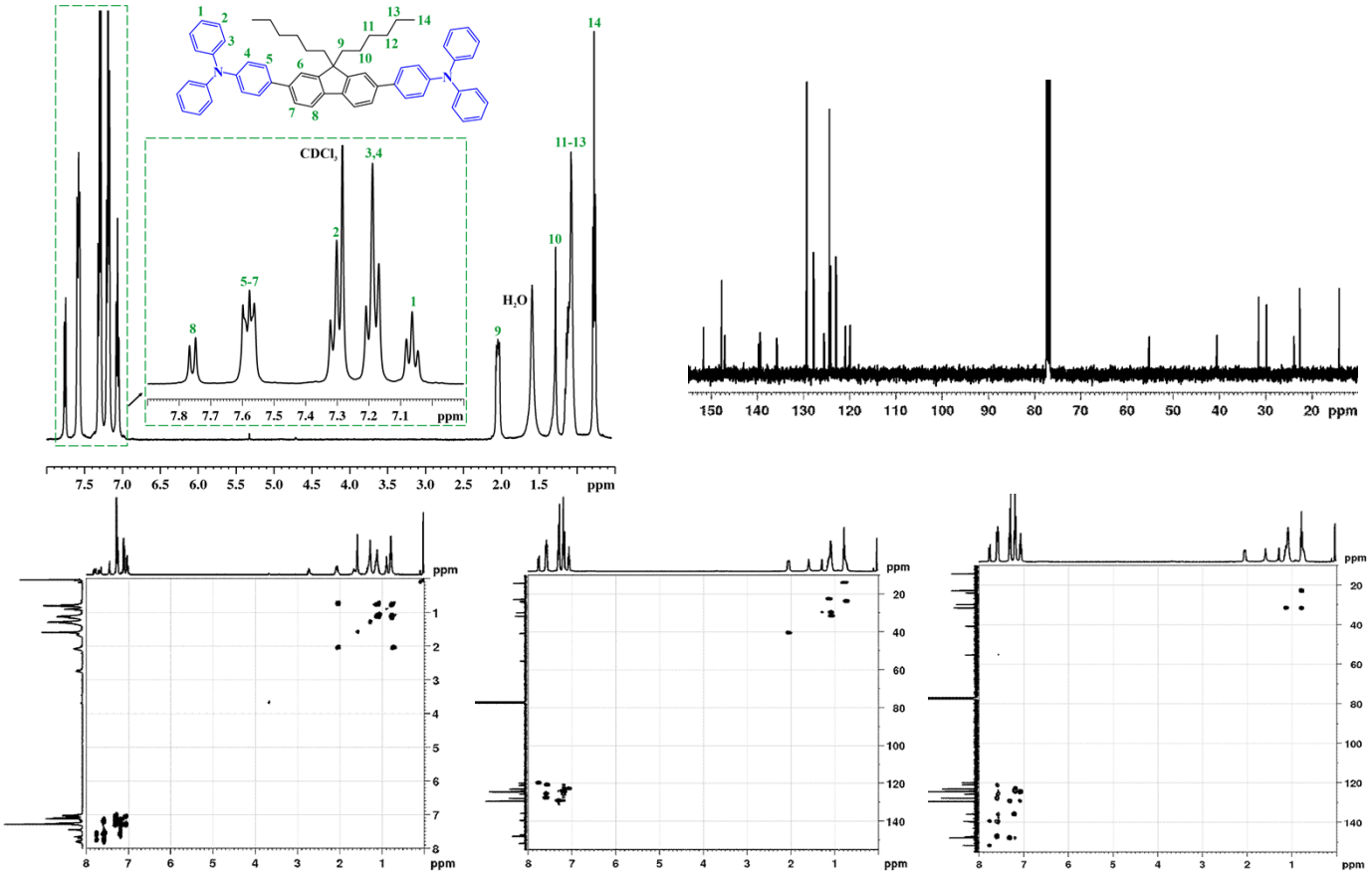

Fig. S1 ^{1}H, ^{13}C (first row, from left to right), COSY, HSQC, and HMBC (second row, from left to right) NMR spectra of **MC1** model compound in $CDCl_3$.

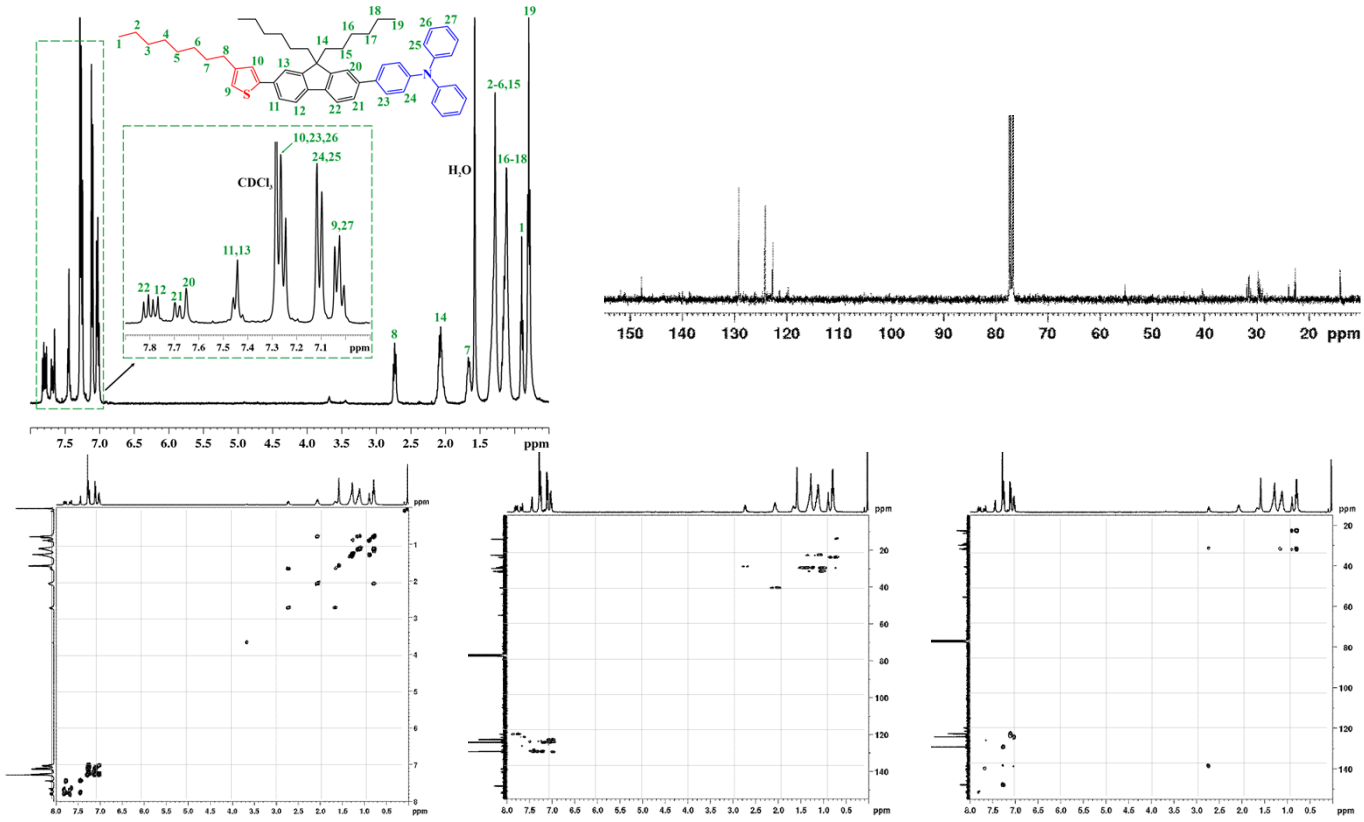

Fig. S2 ^{1}H, ^{13}C (first row, from left to right), COSY, HSQC, and HMBC (second row, from left to right) NMR spectra of **MC2** model compound in $CDCl_3$.

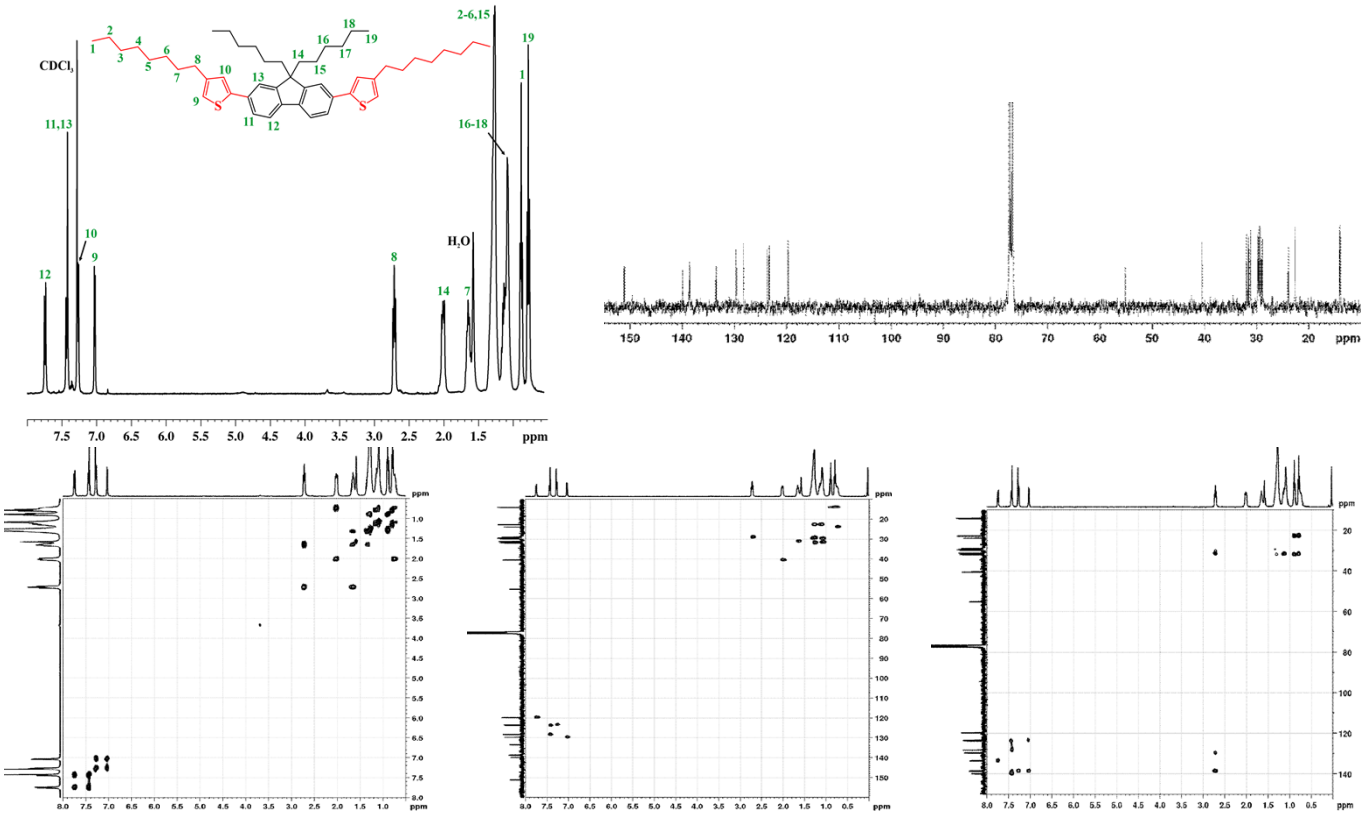

Fig. S3 ^{1}H, ^{13}C (first row, from left to right), COSY, HSQC, and HMBC (second row, from left to right) NMR spectra of **MC3** model compound in $CDCl_3$.

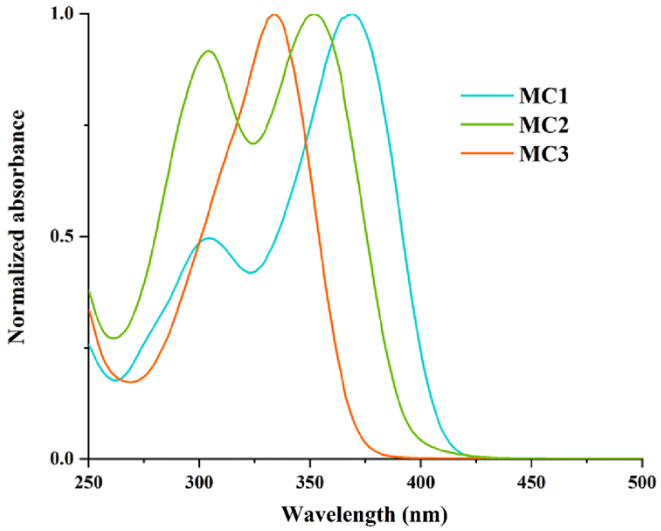

Fig. S4 UV spectra of model compounds.

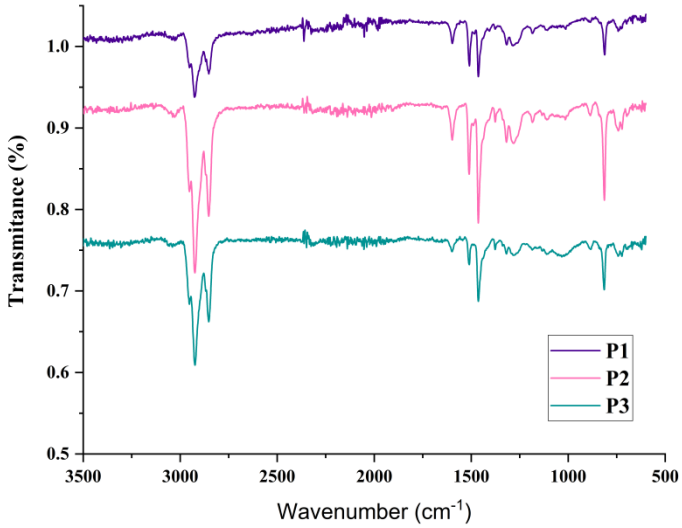

Fig. S5 FT-IR spectra of **P1**–**P3** HBPs.

Table S1 FT-IR shifts of the synthesized polymers.

Band assignment (vibration type)	**P1–P3 wavenumber range** (cm^{-1})
aromatic C–H asymmetric stretching	3070–3017
aliphatic C–H asymmetric stretching	2931–2869
aromatic C=C asymmetric stretching	1601–1597
aromatic C=C symmetric stretching	1510–1515
aliphatic $–CH_2–$ in-plane bending	1466
thiophene C–S–C stretching	1376–1371
aromatic C–N asymmetric stretching	1314

$-CH_3$ in-plane bending	1106
thiophene C–H in-plane deformation/ rocking vibration	1030
aromatic/thiophene C–H out-of-plane bending	812
aromatic C–H (2 neighboring H atoms) out-of-plane bending	738–722
thiophene in-plane deformation	637
thiophene out-of-plane deformation	622

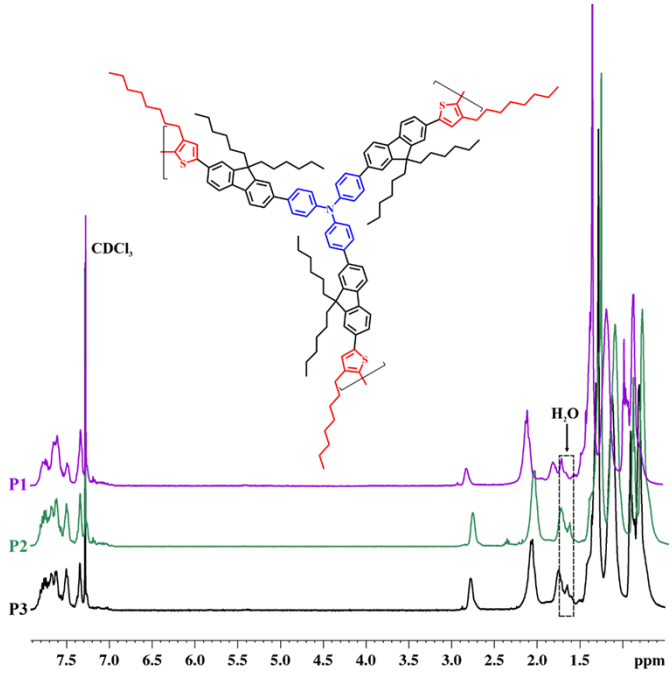

Fig. S6 ^{1}H NMR spectra of hyperbranched polymers **P1**–**P3** in $CDCl_3$.

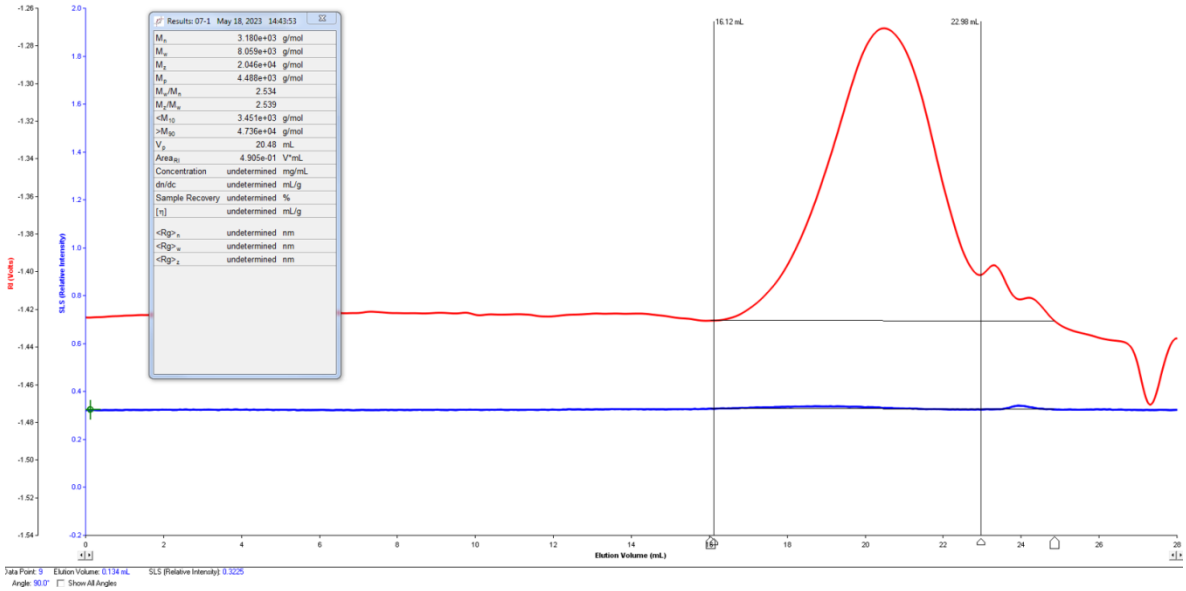

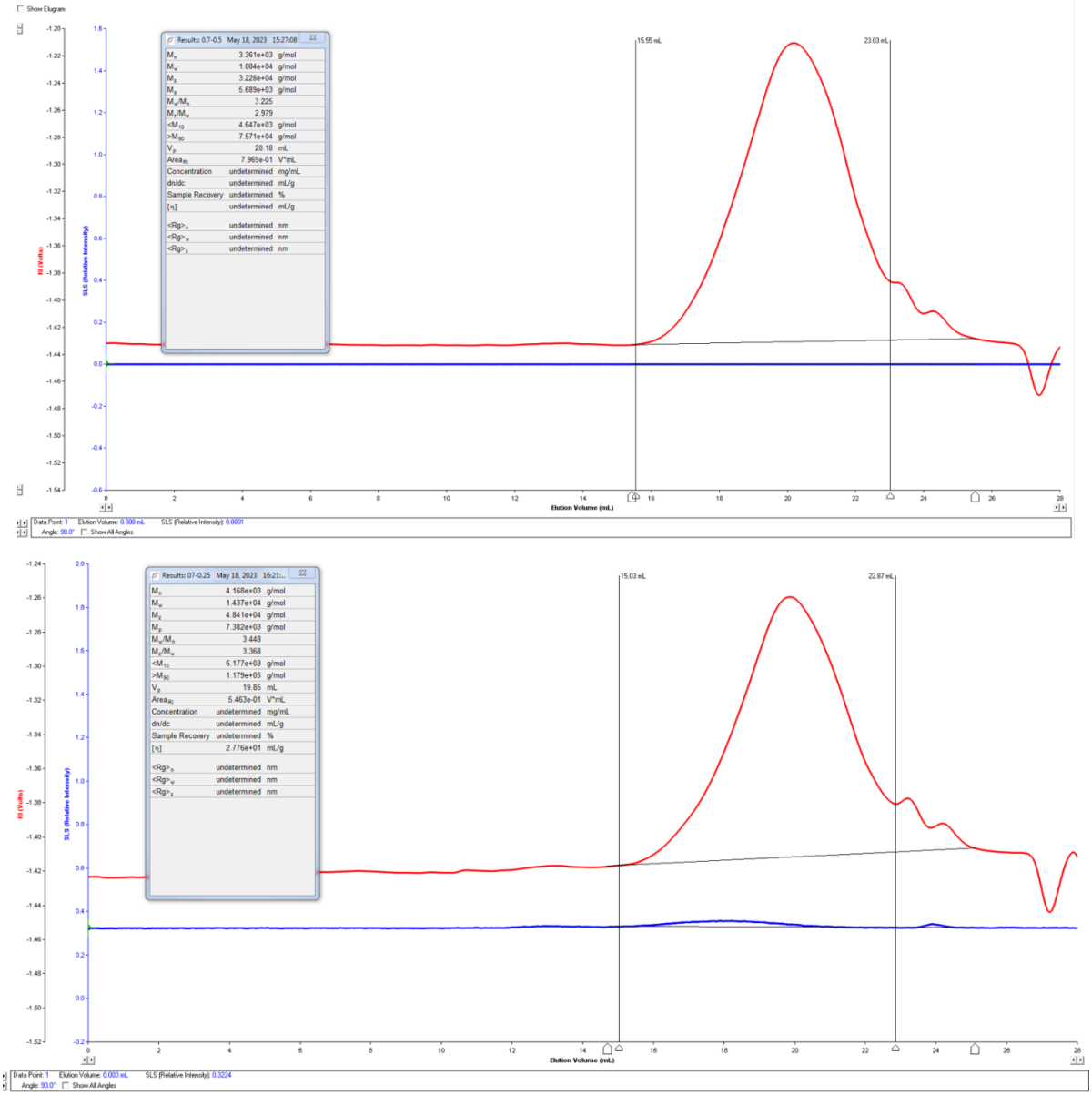

Fig. S7 Raw GPC data of hyperbranched polymers **P1**–**P3** in $CHCl_3$.

Table S2 Molar mass values and solubility of **P1–P3** polymers.

Polymer	M_w	M_w/M_n	Solvent								
	kg·mol^{-1}		$CHCl_3$	DCM	THF	NMP	DMF	DMAc	MeCN	Heptane	Toluene
P1	8.05	2.53	+	+	+	±	±	±	–	±	±
P2	10.8	3.22	+	+	+	±	±	±	–	±	±
P3	14.3	3.44	+	+	+	±	±	±	–	±	±

DCM: dichloromethane; THF: tetrahydrofuran; NMP: *N*-methylpyrrolidone; DMF: *N,N*-dimethylformamide; DMA: *N,N*-dimethylacetamide; MeCN: acetonitrile; +: readily soluble at room temperature; ±: soluble upon additional heating and time; –: not soluble.

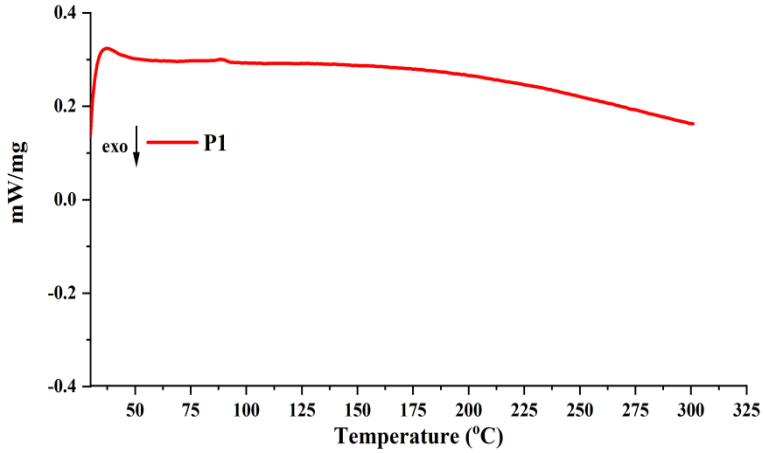

Fig. S8 DSC curve of **P1** hyperbranched polymer.

Polymer	*IDT* (°C)	$T_{10\%}$ (°C)	T_{max} (°C)	W_{700} (%)
P1	414	434	455	62.11
P2	418	438	460	57.85
P3	339 (282, 424)	414	460	54.76

Table S3 Main thermal parameters determined for **P1**–**P3** hyperbranched polymers.

IDT: initial decomposition temperature; $T_{10\%}$: temperature of 10% weight loss; T_{max}: temperature of the maximum decomposition rate; W_{700}: residual weight percentage (char yield) at 700 °C

Table S4 UV–vis absorption and PL maxima of **P1**–**P3** in various solutions.

Media	**P1**			**P2**			**P3**		
	λ_{abs} (nm)	λ_{PL} (nm)		λ_{abs} (nm)	λ_{PL} (nm)		λ_{abs} (nm)	λ_{PL} (nm)	
		$\lambda_{ex}{}^{1}$	$\lambda_{ex}{}^{2}$		$\lambda_{ex}{}^{1}$	$\lambda_{ex}{}^{3}$		$\lambda_{ex}{}^{1}$	$\lambda_{ex}{}^{4}$
toluene	386	456 484^{s} 527^{s}	458 488^{s} 529^{s}	390	460 485^{s} 528^{s}	460 488^{s} 528^{s}	393	461 485^{s} 527^{s}	460 487^{s} 528^{s}
THF	387	455 485^{s}	457 486^{s}	393	459 487^{s} 527^{s}	459 482^{s} 534^{s}	394	459 488^{s} 527^{s}	459 487^{s} 534^{s}
DCM	389	457 488^{s} 520^{s}	458 486^{s} 524^{s}	394	459 491^{s} 527^{s}	460 488^{s} 528^{s}	396	461 488^{s} 528^{s}	461 487^{s} 528^{s}

DMF	390	–	–	392	–	–	397	–	–
		462	462		460	460		463	463
NMP	393	484[s]	485[s]	395	486[s]	484[s]	396	488[s]	486[s]
		519[s]	523[s]		523[s]	526[s]		523[s]	525[s]
NMP Φ_{PL} (%)		44.5			33.4			28.8	
simulated	–	–	–	–	–	–	435.4 435.2 360.92 360.9 359.67 320.96	–	–

λ_{abs}: wavelength of the UV–vis absorption maximum; λ_{PL}: wavelength of the PL maximum; λ_{ex}^{1}: 295 nm; λ_{ex}^{2}: 385 nm; λ_{ex}^{3}: 390; λ_{ex}^{4}:395; s: shoulder; Φ_{PL}: absolute fluorescence quantum yields

Table S5 UV–vis absorption and PL maxima of **P1**–**P3** films obtained from various solvents.

Film drop-cast from	**P1**		**P2**		**P3**	
	λ_{abs} (nm)	λ_{PL} (nm)	λ_{abs} (nm)	λ_{PL} (nm)	λ_{abs} (nm)	λ_{PL} (nm)
toluene	–	493 527[s]	–	493	–	487
THF	394	488	397	492	400	490
DCM	391	491	400	508	405	493
NMP	393	495	396	492	400	502
toluene Φ_{PL} (%)	0.9		1.7		0.5	

λ_{abs}: wavelength of the UV–vis absorption maximum; λ_{PL}: wavelength of the PL maximum (λ_{ex}: 400 nm); s: shoulder; Φ_{PL}: absolute fluorescence quantum yields

Table S6 CIE values of **P1**–**P3** solutions in various solvents (at different excitation wavelengths) and as films drop-cast from toluene.

P1				**P2**				**P3**			
NMP	**Toluene**	**THF**	**DCM**	**NMP**	**Toluene**	**THF**	**DCM**	**NMP**	**Toluene**	**THF**	**DCM**
385 nm				**390 nm**				**395 nm**			
x: 0.17	x: 0.15	x: 0.16	x: 0.17	x: 0.16	x: 0.15	x: 0.15	x: 0.17	x:0.14	x: 0.15	x: 0.16	x:0.17

y: 0.23	y: 0.18	y: 0.17	y: 0.2	y: 0.22	y: 0.21	y: 0.2	y: 0.22	y: 0.2	y: 0.22	y: 0.21	y:0.24

film

400 nm

x: 0.31	x: 0.19	x: 0.21	x: 0.22	x: 0.3	x: 0.2	x: 0.24	x: 0.3	x: 0.28	x: 0.18	x: 0.19	x: 0.27
y: 0.46	y: 0.45	y: 0.42	y: 0.46	y: 0.44	y: 0.46	y: 0.46	y: 0.56	y: 0.43	y: 0.43	y: 0.4	y: 0.51

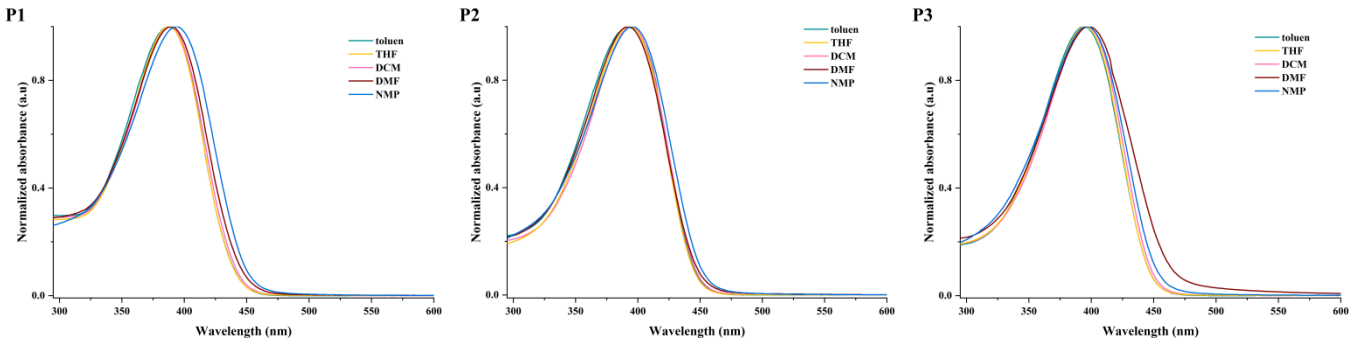

Fig. S9 UV–vis absorption spectra of **P1**–**P3** in various solutions.

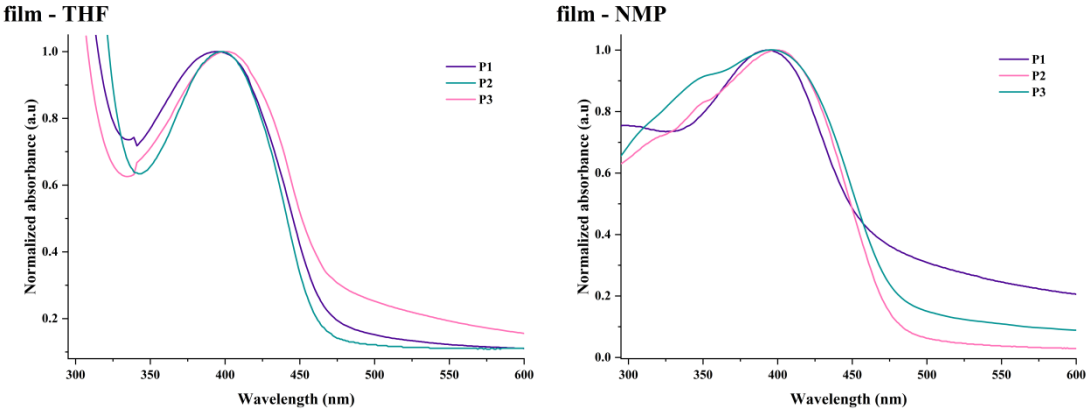

Fig. S10 UV–vis absorption spectra of **P1**–**P3** thin films obtained from THF or NMP.

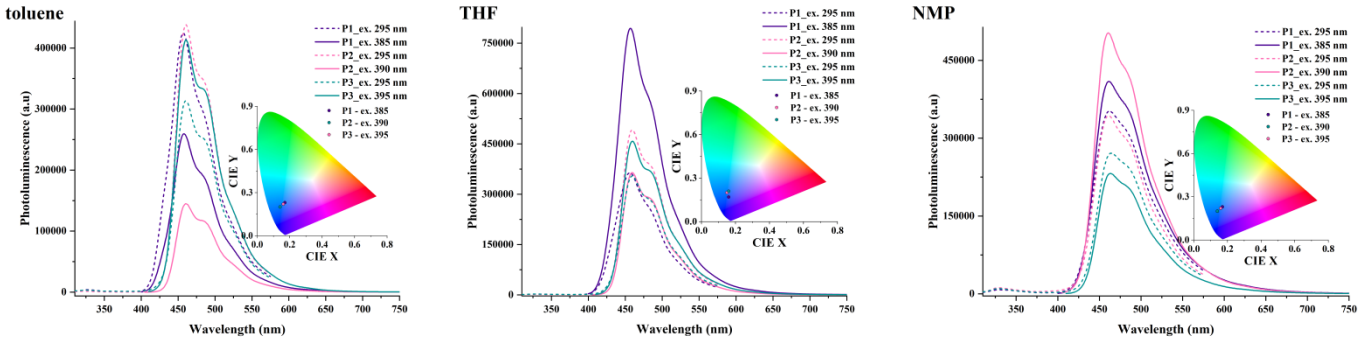

Fig. S11 PL spectra of **P1**–**P3** solutions in various solvents as a function of excitation wavelength.

Insets: associated chromaticity diagrams.

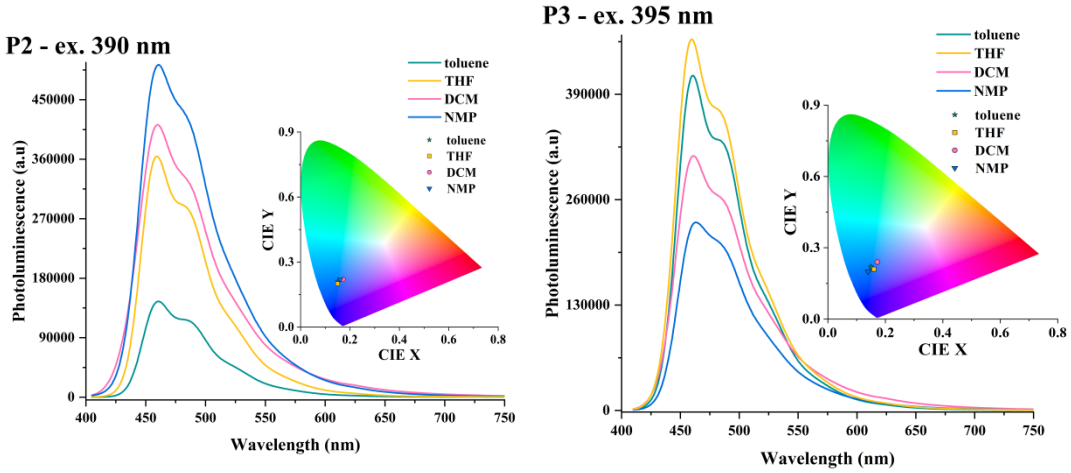

Fig. S12 PL spectra of **P2** and **P3** solutions in various solvents at the same excitation wavelength. Insets: associated chromaticity diagrams.

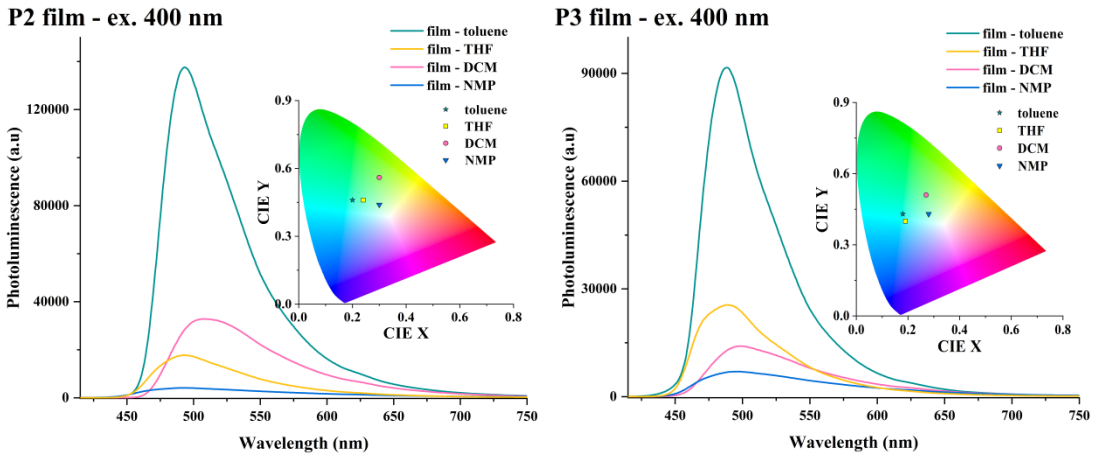

Fig. S13 PL spectra of **P2** and **P3** thin films obtained from various solvents. Insets: associated chromaticity diagrams.

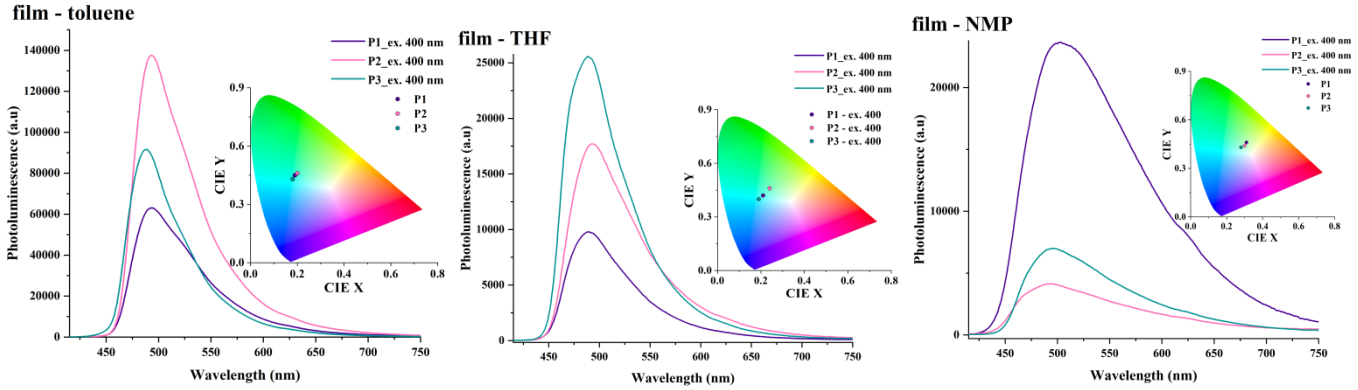

Fig. S14 PL spectra of **P1**–**P3** films obtained from various solvents.

Insets: associated chromaticity diagrams.

Table S7 Redox potentials and energy levels of the polymers **P1**–**P3**.

Polymer	λ_{onset}[a] (nm)	Oxidation potential[b] (V)		Energy levels (eV)					
		E_{onset}^{ox}	E^{ox}	E_{HOMO}		E_{LUMO}		E_g	
				exp.	cal.	exp.	cal.	exp.	cal.
P1	454	0.54	0.73 0.95	-5.01	-5.02	-2.27	-1.80	2.73	3.22
P2	464	0.61	1.02	-5.08		-2.4		2.67	
P3	458	0.76	0.89	-5.23		-2.52		2.7	

[a] λ_{onset} determined from the intersection of the UV-vis and PL spectra of films obtained from DCM; [b] values from CV curves

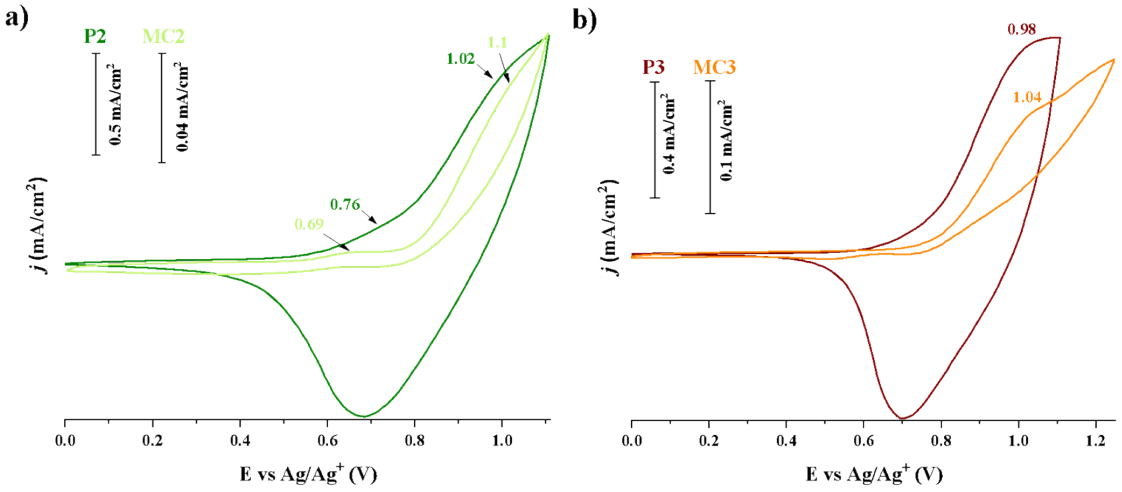

Fig. S15 Comparative cyclic voltammetry curves of **P2**-**MC2 (a)** and **P3**-**MC3 (b)** pairs.

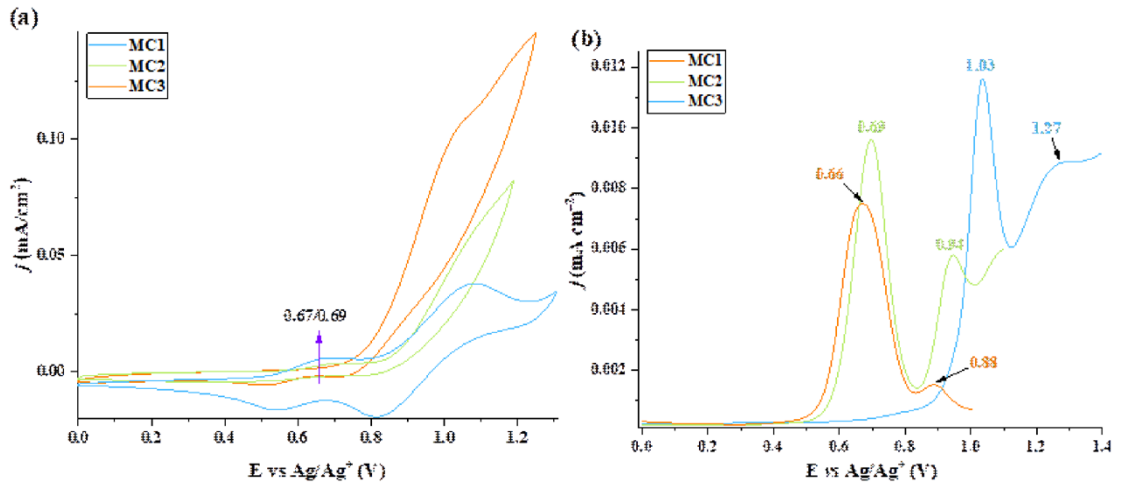

Fig. S16 Comparative cyclic voltammetry **(a)** and differential pulse voltammetry **(b)** curves of **MC1**–**MC3**.

References

1 H. Diliën, A. Palmaerts, M. Lenes, B. de Boer, P. Blom, T. J. Cleij, L. Lutsen and D. Vanderzande, *Macromolecules*, 2010, **43**, 10231–10240.

2 H. Tanaka, K. Shizu, H. Nakanotani and C. Adachi, *The Journal of Physical Chemistry C*, 2014, **118**, 15985–15994.

3 L. S. Rohwer and J. E. Martin, *J Lumin*, 2005, **115**, 77–90.

4 C. H. Ng, T. S. Ripolles, K. Hamada, S. H. Teo, H. N. Lim, J. Bisquert and S. Hayase, *Sci Rep*, 2018, **8**, 2482.

5 A. M. Wallace, C. Curiac, J. H. Delcamp and R. C. Fortenberry, *J Quant Spectrosc Radiat Transf*, 2021, **265**, 107544.

6 S. Prasad, R. H. Alhandel, N. N. Asemi and M. S. AlSalhi, *Polymers (Basel)*, 2023, **15**, 4572.